

Novel Decellularization Scheme for Preparing Acellular Fish Scale Scaffolds for Bone Tissue Engineering

Shilong Su, Ruideng Wang, Jinwu Bai, Zhengyang Chen, and Fang Zhou*

Cite This: *ACS Omega* 2025, 10, 230–238

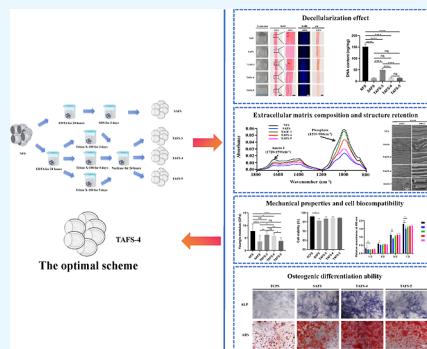
Read Online

ACCESS |

Metrics & More

Article Recommendations

ABSTRACT: In bone tissue engineering, a suitable scaffold is the key. Due to their similar composition to bone tissue, special structure, good mechanical properties, and osteogenic properties, acellular fish scale scaffolds are potential scaffolds for bone tissue engineering. At present, the fish scale decellularization scheme mostly uses a combination of sodium dodecyl sulfate and ethylenediamine tetraacetic acid (EDTA), but this method has problems. We optimized this method using a combined method of Triton X-100, EDTA, and nuclease. In this study, the optimal scheme was screened with respect to the decellularization effect, extracellular matrix composition and structure retention, mechanical properties, cell biocompatibility, and osteogenic differentiation ability. The results showed that the optimal scheme was as follows: the native fish scales were incubated in 0.1% EDTA for 24 h, and then the cellular components were removed with 1% Triton X-100 for 4 days, followed by nuclease digestion for 24 h. On that basis, we proposed a novel and more suitable fish scale decellularization scheme, and the acellular fish scale scaffold prepared by this decellularization scheme may have great potential in bone tissue engineering.



INTRODUCTION

Bone tissue engineering is a complex process, including cell migration, proliferation, differentiation, matrix formation, and bone remodeling.¹ In bone tissue engineering, a suitable scaffold is the key.² In recent years, natural acellular matrix materials have aroused great interest in the field of tissue engineering because of their ability to construct biomimetic scaffolds with low immunogenicity and high biocompatibility.^{3,4} These scaffolds show a variety of physiological functions, such as a repository of cytokines, which transmits specific signals through interactions with cell surface receptors and provides a natural microenvironment to regulate the biological activity of interacting cells.^{3–5}

As the natural leather armor of fish, fish scales can not only protect fish from a variety of natural enemies but also ensure unlimited swimming of fish in the water. In recent years, fish scales have attracted more and more attention in tissue engineering because of their special composition and structure. Fish scales are mainly composed of hydroxyapatite and type I collagen, and their proportion is similar to that of bone tissue.⁶ The layers of collagen fibers with different orientations form a special “Bouligand” structure, which gives fish scales excellent mechanical properties through the deformation coordination mechanism.⁷ Fish scales also have excellent biocompatibility, low immunogenicity,⁸ and the ability to enhance cell adhesion, promote cell proliferation, and induce differentiation.⁹ Fish scales have been used as scaffolds for bone tissue engineering to repair and regenerate bone defects, and good results have been achieved.^{9,10} The earth is rich in fish resources, but in the

process of fish processing, due to the lack of commercial value, a large number of fish scales are discarded, resulting in a serious waste of natural resources and environmental problems. Using fish scales as a biodegradable and cheap biological resource for tissue engineering is a kind of resource reuse. Based on these advantages, acellular fish scale scaffolds are potential scaffolds for bone tissue engineering.

At present, most of the decellularization methods reported in the literature use ionic detergent sodium dodecyl sulfate (SDS) combined with ethylenediamine tetraacetic acid (EDTA) to decellularize fish scales.^{9,10} Although SDS has a good decellularization effect, it can highly destroy the microstructure of the extracellular matrix and protein activity in tissue.^{11–13} In addition, the ionicity and cytotoxicity of SDS, as well as the difficulty of completely removing SDS from acellular tissue, may affect the cell biocompatibility in the acellular matrix scaffold.^{12–14} As a nonionic cell detergent, TritonX-100 is a mild decellularization agent that has been widely used to prepare biological decellularized matrix scaffolds,¹⁵ which destroys the interaction between lipids and lipoproteins to decellularize while keeping the interaction

Received: May 30, 2024

Revised: December 12, 2024

Accepted: December 16, 2024

Published: January 1, 2025



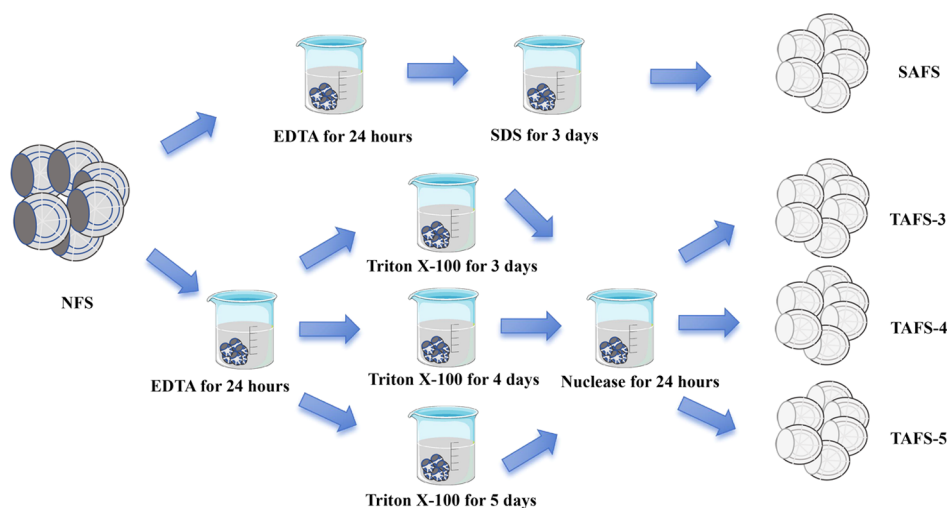


Figure 1. Schematic diagram of the process to prepare acellular fish scale scaffolds. NFS: native fish scales; EDTA: ethylenediamine tetraacetic acid; SDS: sodium dodecyl sulfate; SAFS: SDS-treated acellular fish scale scaffolds; TAFS: Triton X-100-treated acellular fish scale scaffolds.

between proteins unchanged.¹⁶ Nucleases are endonucleases that hydrolyze DNA and ribonucleic acid chains. Generally, if effective decellularization cannot be achieved using nonionic cell scavengers alone, adding these enzyme preparations to the detergent can more effectively remove residual DNA.¹⁷ To solve these problems, we decided to optimize the existing decellularization scheme of fish scales, adopt the combined method of Triton X-100, EDTA, and nuclease, and verify whether the new method has more advantages than the previous method. This study was evaluated from the aspects of the decellularization effect, extracellular matrix composition and structure retention, mechanical properties, cell biocompatibility, and osteogenic differentiation ability.

MATERIALS AND METHODS

Materials. The healthy Grass carps (age: 2 years, weight: 1 kg, body length: 20 cm) were obtained from a commercial dealer in Beijing. Tris-hydrochloride (Tris-HCl), SDS, Triton X-100, EDTA, and ribonuclease A were procured from Bioroyee Inc. (Beijing, China). Deoxyribonuclease I was procured from Mreda (Beijing, China). Rat bone mesenchymal stem cells (BMSCs) were obtained from Procell Life Science and Technology Co., Ltd. (Beijing, China).

Decellularization of Fish Scales. Larger scales (2–3 cm in diameter) were chosen and washed with running tap water. Forceps and scalpels were used to remove their epidermis, fascia, and other soft tissue, and they were rinsed again with distilled water 5 times.

For SDS-treated acellular fish scale scaffolds (SAFS), we used the method reported in the literature.^{9,10} The native fish scales (NFS) were incubated in 10 mM Tris-HCl buffer and 0.1% EDTA at 4 °C for 24 h, and then the cellular components in the fish scales were removed with 0.1% SDS at 4 °C for 3 days and washed with distilled water for 5 times. Finally, the acellular fish scales were sterilized with 75% ethanol, freeze-dried, and stored for later use.

For Triton X-100-treated acellular fish scale scaffolds (TAFS), we used the combined method of EDTA, Triton X-100, and nuclease. Referring to the reagent types and concentrations reported in the literature,^{15,18,19} we conducted preliminary experiments and finally determined the decellularization steps as follows. NFS was incubated in 10 mM Tris-

HCl buffer and 0.1% EDTA at 4 °C for 24 h, and then the cellular components of the fish scales were removed with 1% Triton X-100 at 4 °C for 3, 4, and 5 days, respectively. After that, the fish scales were digested with nuclease solution (containing 500 U/mL deoxyribonuclease I and 1 mg/mL ribonuclease A) at 37 °C for 24 h and washed with distilled water 5 times. Finally, the acellular fish scales were sterilized with 75% ethanol, freeze-dried, and stored for later use. According to the different Triton X-100 treatment times, the three groups of scaffolds were named TAFS-3, TAFS-4, and TAFS-5, respectively (Figure 1).

Histological Evaluation. The scaffolds before or after decellularization were embedded in paraffin and sectioned longitudinally at a thickness of 5 μm. Hematoxylin and eosin (H&E) staining, 4',6-diamidino-2-phenylindole (DAPI) staining, and picosirius red (PR) staining were used to qualitatively evaluate the decellularization effect and extracellular matrix retention.

Content of Hydroxyapatite and Collagen. The scaffolds before or after decellularization were embedded in paraffin and sectioned longitudinally at a thickness of 7 μm. After vacuum drying overnight and dewaxing, the slices were evaluated by Fourier transform infrared spectroscopy (FTIR) (Thermo Fisher Scientific, USA) to obtain infrared spectra.^{20,21} According to the literature,^{21–23} the peak areas of phosphate (1200–900 cm⁻¹) and amide I (1720–1590 cm⁻¹) in infrared spectra were respectively calculated to semi-quantitatively characterize the contents of hydroxyapatite and collagen of scaffolds ($n = 5$).

DNA Residence Analysis. To quantitatively compare the decellularization effect, according to the manufacturer's instructions, the total DNA in NFS, SAFS, and TAFS ($n = 5$) was extracted using a marine animal tissue genomic DNA extraction kit (Bioroyee, China). Finally, the DNA content was calculated by a spectrophotometer (DHS, China).

Scanning Electron Microscopy. The scaffolds before or after decellularization were freeze-dried and sputter-coated with gold before observation. The surface microstructure of NFS, SAFS, and TAFS ($n = 5$) was observed with scanning electron microscopy (SEM) (JSM-7900F, JEOL, Japan). During SEM observation, scaffolds were also examined by

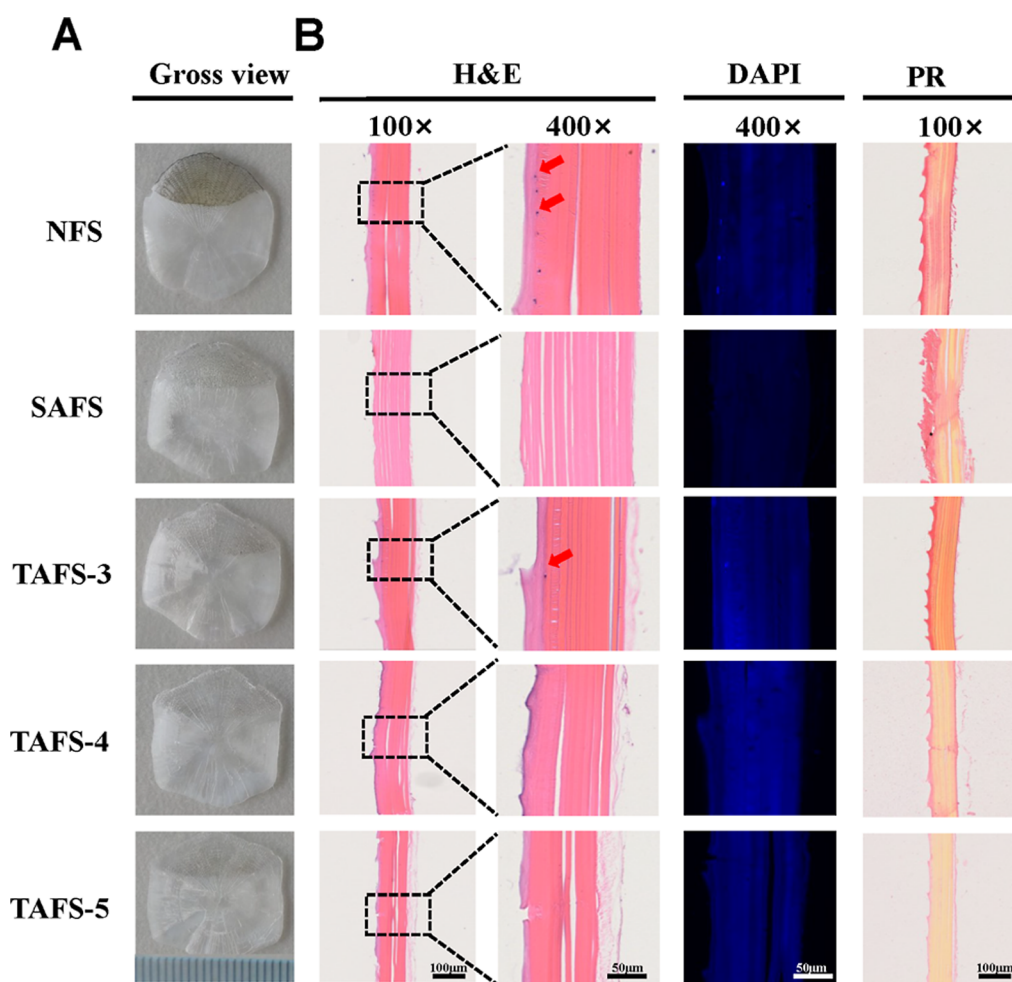


Figure 2. (A) Macroscopic features of NFS, SAFS, and TAFS. (B) Histological evaluation of NFS, SAFS, and TAFS. Sections stained with H&E, DAPI, and PR. Scale bar = 100 μm . HE: Hematoxylin and eosin; DAPI: 4',6-diamidino-2-phenylindole; PR: picosirius red; NFS: native fish scales; SAFS: SDS-treated acellular fish scale scaffolds; TAFS: Triton X-100-treated acellular fish scale scaffolds.

using energy-dispersive X-ray spectroscopy (EDS) elemental mapping.

Water Absorption Capacity. The swelling behavior of the scaffolds was evaluated by immersing the freeze-dried scaffolds in phosphate buffered saline (PBS) (PH = 7.4) at 37 $^{\circ}\text{C}$ for 48 h ($n = 5$). The swelling rate was calculated as follows

$$\text{Swelling rate} = (W_w - W_d) / W_d \times 100\%$$

where W_d is the initial weight of the freeze-dried sample, and W_w is the weight of the swollen sample.

In Vitro Degradation. The degradation of the scaffolds was evaluated by the gravimetric method. The freeze-dried scaffolds were incubated in PBS (PH = 7.4) at 37 $^{\circ}\text{C}$, and PBS was replaced every 3 days ($n = 5$). At 2, 4, 6, and 8 weeks, the liquid was removed and freeze-dried, and the remaining scaffolds were weighed. The degradation rate was calculated as follows

$$\text{Degradation rate} = (W_0 - W_t) / W_0 \times 100\%$$

where W_0 is the initial weight of the freeze-dried sample, and W_t is the weight of the remaining sample.

Mechanical Performance Test. The mechanical performance test was performed by atomic force microscopy (AFM) (Bruker, Germany). Before the test, the scaffold was fixed to the sample stage ($n = 5$); five randomly different 10 $\mu\text{m} \times 10$

μm areas on each sample were measured, and the force–displacement curves were collected. The force–displacement curve was fitted by the Hertzian model using NanoScope Analysis software (Version 3.0, Bruker, Germany) to determine Young's modulus of the scaffolds.

In Vitro Biocompatibility. Cell Viability. The calcein-AM/propidium iodide (PI) kit (Servicebio, China) was used to observe the cell viability of the scaffolds. Considering that the scaffolds are not transparent to light and the effect of the scaffold on the adsorption of the working liquid, we obtained images of cells co-cultured with the scaffolds rather than images of cells on the scaffolds. Briefly, scaffolds were cut into cuboids (about 5 \times 5 \times 0.5 mm). BMSCs (2×10^4 cells, Passage 4) were co-cultured with SAFS, TAFS, or tissue culture polystyrenes (TCPS) (as control) ($n = 3$) and placed in a 48-well culture plate. After the 3 day culture, cells were washed with PBS 3 times and incubated with the working liquid according to the manufacturer's recommendations at 37 $^{\circ}\text{C}$ for 20 min. Then the working liquid was removed. The images were captured with a fluorescence microscope (Leica, Germany). Cell viability was calculated as follows: (live cells/total cells) \times 100%.

Cell Proliferation. The cell proliferation was quantified by the cell counting kit-8 (CCK-8) test (Fude Biological, China) on BMSCs. Briefly, BMSCs (2×10^4 cells, Passage 4) were

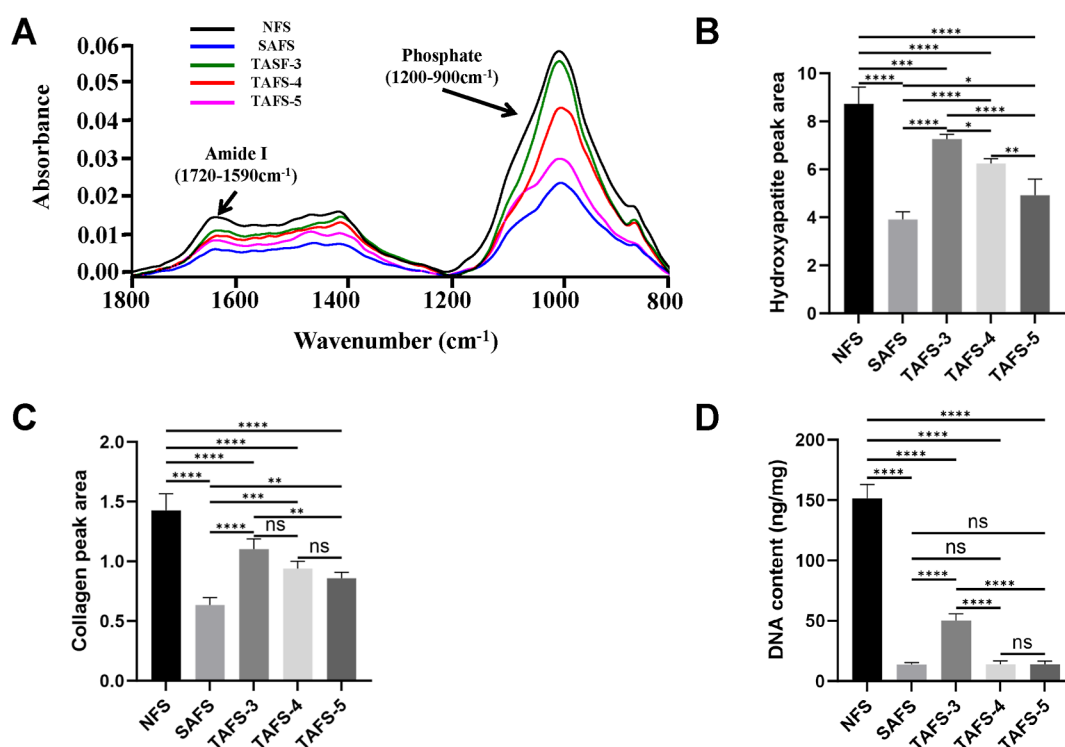


Figure 3. (A) Characteristic FTIR spectrum for NFS, SAFS, and TAFS, and note the amide I peak and the phosphate peak are, respectively, indicative of collagen and hydroxyapatite. Hydroxyapatite (B), collagen (C), and DNA (D) contents of NFS, SAFS, and TAFS. All values are presented as means \pm standard deviation (* $P < 0.05$, ** $P < 0.01$, *** $P < 0.001$, ns: $P > 0.05$). NFS: native fish scales; SAFS: SDS-treated acellular fish scale scaffolds; TAFS: Triton X-100-treated acellular fish scale scaffolds.

seeded onto SAFS, TAFS, or TCPS (as control) ($n = 5$). After 1, 3, 5, and 7 day cultures, the medium was removed, and the CCK8 working solution was added to assess the cell proliferation according to the instructions. Then, the absorbance at 450 nm of the supernatant was measured with a microplate reader (Molecular Devices, USA).

In Vitro Osteogenic Differentiation. Considering that TAFS-3 did not meet the minimum requirements for successful decellularization, we evaluated only the osteogenic differentiation abilities of SAFS, TAFS-4, and TAFS-5. In this study, BMSCs were co-cultured with scaffolds to measure alkaline phosphatase (ALP) activity and calcium deposition to compare and evaluate their osteogenic inducibilities.

ALP Activity and Alizarin Red Staining. BMSCs (1×10^4 cells, Passage 3) were seeded onto SAFS, TAFS-4, TAFS-5, and TCPS (as control) for 24 h ($n = 3$), and then the medium was replaced with osteogenic medium, which was replaced every 2 days. After 7 and 14 days, cells were fixed with 4% paraformaldehyde and then stained using an ALP staining kit (Beyotime, China) and Alizarin Red Staining (ARS) kit (Beyotime, China), respectively. We first took an overall image of each well with a camera, and then more detailed images were captured by a microscope (Nikon, Japan). Similarly, considering that the scaffolds are not transparent to light and the effect of the scaffold on the adsorption of the working liquid, we obtained detailed images of cells co-cultured with the scaffolds rather than images of cells on the scaffolds. In addition, the ALP activity was measured using an ALP assay kit (Beyotime, China). The measured ALP activity was normalized to the total intracellular protein content, which was measured using a BCA protein assay kit (Beyotime, China).

Statistical Analysis. The analyses were performed using SPSS software (Version 25.0, SPSS, USA). The quantitative data were expressed as mean \pm standard deviation. Student's *t*-test was used for the comparison between the two groups. One-way ANOVA with a post hoc test was used for multiple-group comparisons. If the data were not normally distributed, nonparametric tests were used. $P < 0.05$ was considered statistically significant.

RESULTS

Characteristics of Scaffolds. Macroscopic Observation. The selected fish scales were translucent and irregularly round, about 2 cm in diameter. One side of the NFS was covered with oval dark brown fish skin, covering about a quarter of its area. The surface of the NFS had ridges and grooves arranged regularly in a radial or annular manner. After a series of decellularization processes, acellular fish scale scaffolds were prepared. Compared with NFS, the surface-covered fish skin was removed and the acellular fish scale scaffolds became lighter and more transparent, but the regularly arranged ridges and grooves on the surface were retained (Figure 2A).

Histological Evaluation. As shown in Figure 2B, H&E, DAPI, and PR staining were used to evaluate the decellularization effect of fish scales and the preservation of extracellular matrix components, such as collagen. Extensive nuclear staining could be seen in the H&E or DAPI staining of NFS. The cellular components in SAFS were completely removed. In TAFS, Triton X-100 treatment for 3 days could not completely remove the cellular components of the scaffolds, while extending the treatment time to 4 and 5 days could completely remove the nuclei of the scaffolds. All scaffolds showed extensive collagen staining, but all decellu-

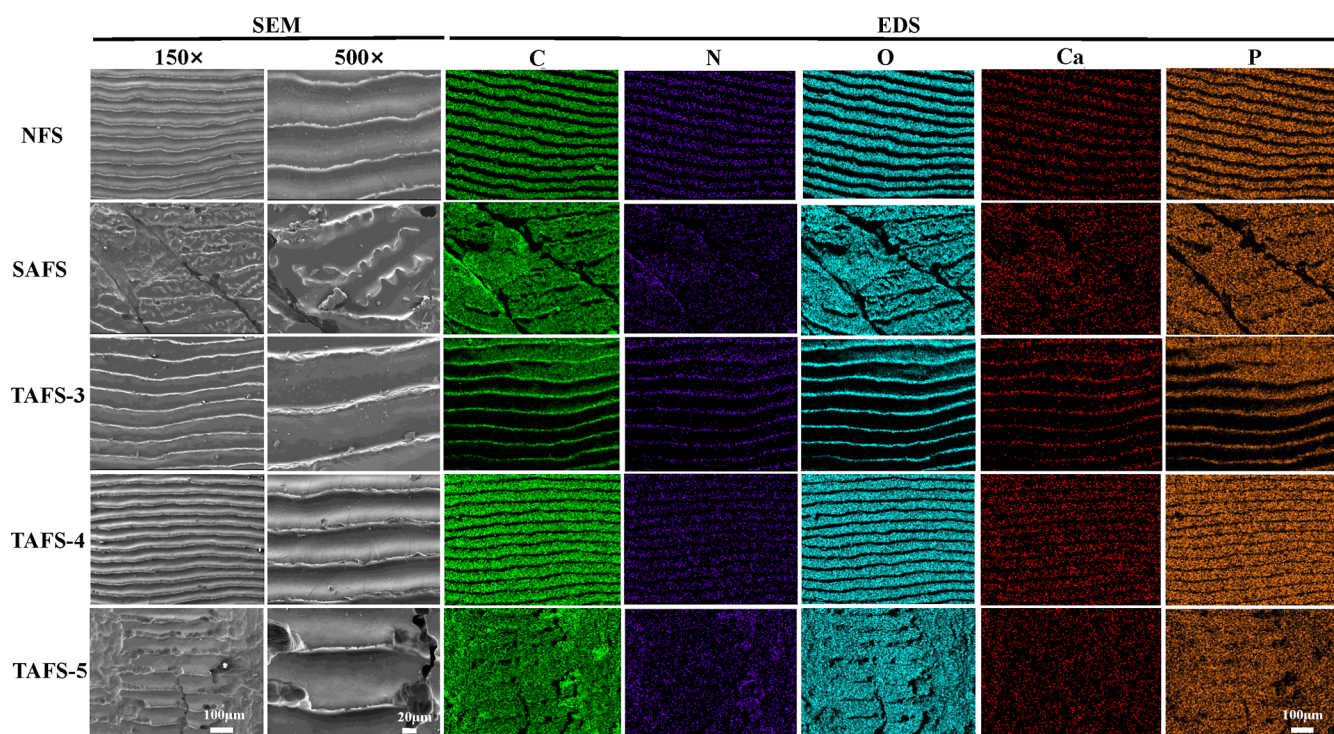


Figure 4. SEM and EDS elemental mapping images of NFS, SAFS, and TAFS. Scale bar = 100 μm . SEM: scanning electron microscopy; EDS: energy-dispersive X-ray spectroscopy; NFS: native fish scales; SAFS: SDS-treated acellular fish scale scaffolds; TAFS: Triton X-100-treated acellular fish scale scaffolds.

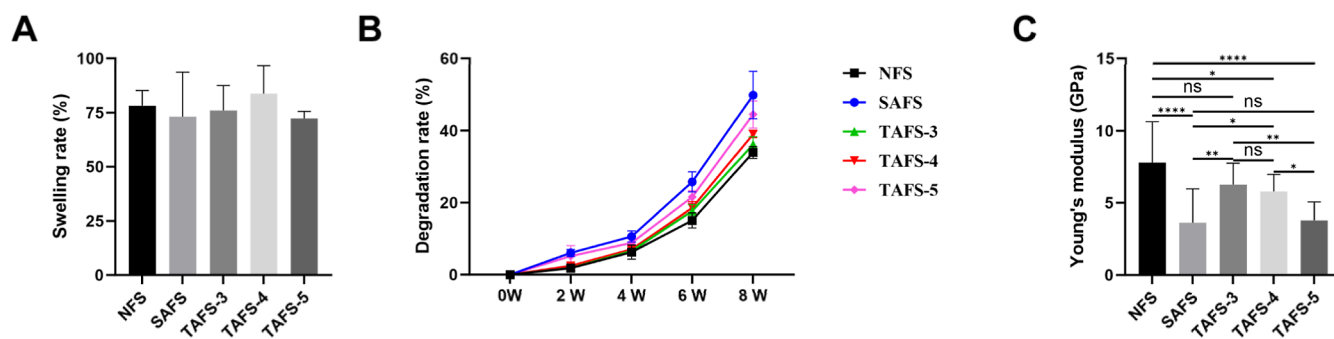


Figure 5. Swelling rates (A), degradation rates at 2 weeks, 4 weeks, 6 weeks, and 8 weeks (B), and Young's modulus (C) of NFS, SAFS, and TAFS. All values are presented as means \pm standard deviation (* $P < 0.05$, ** $P < 0.01$, *** $P < 0.001$, ns: $P > 0.05$). NFS: native fish scales; SAFS: SDS-treated acellular fish scale scaffolds; TAFS: Triton X-100-treated acellular fish scale scaffolds.

rization treatments more or less reduced collagen staining. The collagen staining of TAFS-3 and TAFS-4 decreased slightly, while the staining of SAFS and TAFS-5 decreased significantly. In addition, we also found that TAFS-3 and TAFS-4 were more effective in preserving the microstructure of fish scales.

Content of Hydroxyapatite and Collagen. Hydroxyapatite and collagen are the main extracellular matrix components of the fish scales. We innovatively applied FTIR to quantitatively evaluate the content of hydroxyapatite and collagen in the scaffolds (Figure 3). After a series of decellularization processes, the scaffolds' hydroxyapatite and collagen contents were reduced. For hydroxyapatite in scaffolds, its content decreased by about 55.16% in SAFS, 16.84% in TAFS-3, 28.47% in TAFS-4, and 43.60% in TAFS-5 compared with NFS. For collagen in scaffolds, SAFS, TAFS-3, TAFS-4, and TAFS-5, respectively, lost about 55.49%, 22.73%, 34.08%, and 39.91% of the collagen content with respect to

NFS. Overall, TAFS-3 and TAFS-4 had better effects in retaining extracellular matrix components in fish scales.

DNA Residence. The DNA content of NFS was 151.45 ± 11.51 ng/mg (dry weight). After a series of decellularization processes, the DNA contents of the scaffolds were significantly reduced. The DNA content of TAFS-3 was 50.15 ± 5.63 ng/mg. The DNA contents of SAFS, TAFS-4, and TAFS-5 were all less than 50 ng/mg (Figure 3D).

SEM. SEM was used to observe the surface microstructural changes of the scaffolds before and after decellularization (Figure 4). The surface of the NFS had a directional microstructure, which was characterized by regularly arranged ridges and grooves. After decellularization, the surface microstructure of TAFS-3 and TAFS-4 was preserved intact, while the surface microstructures of SAFS and TAFS-5 were destroyed, of which SAFS was destroyed most obviously. EDS elemental mapping was used to analyze the distribution of C, N, O, Ca, and P elements on the surface of the scaffolds

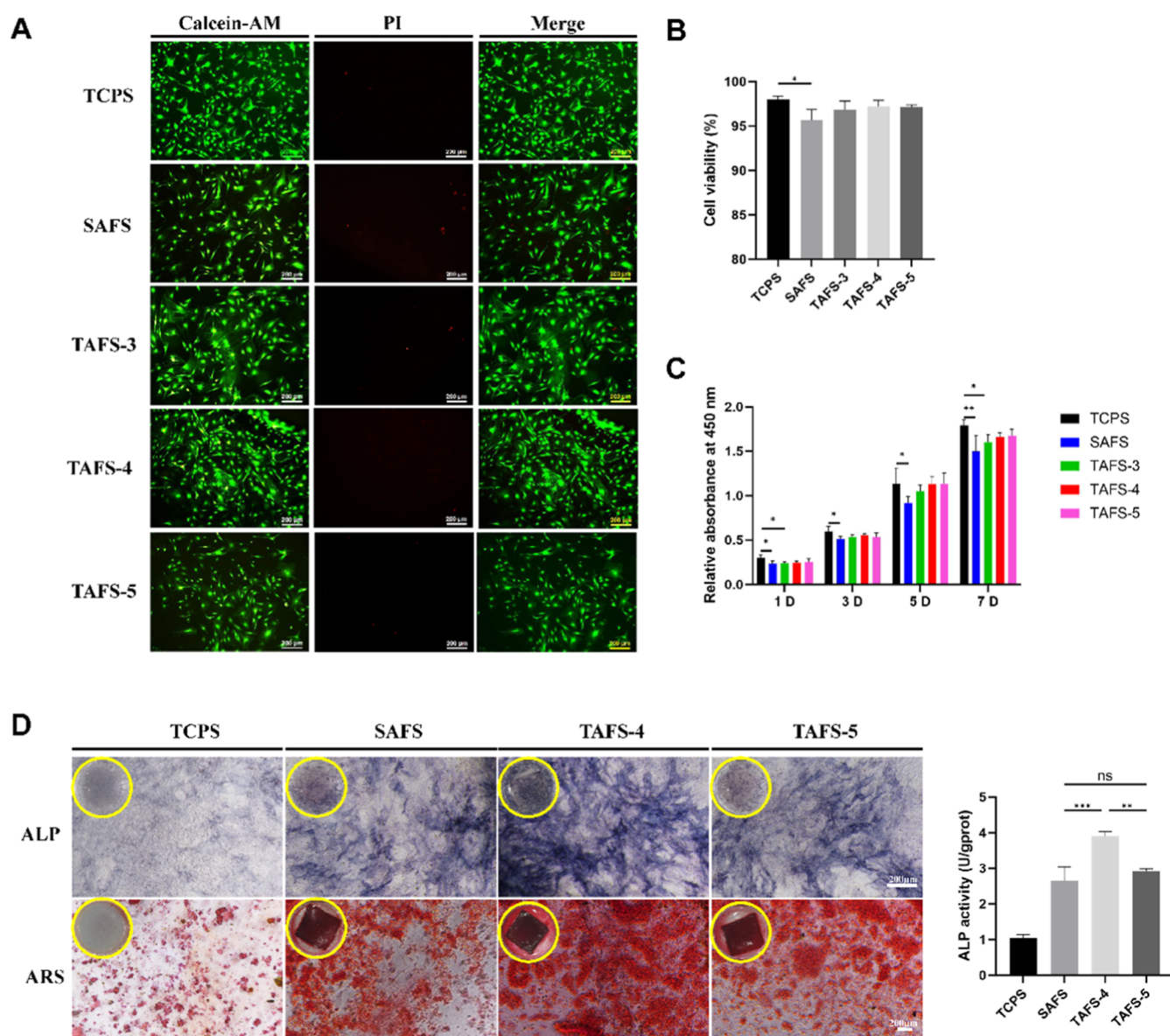


Figure 6. (A) Calcein-AM/PI staining of TCPS, SAFS, and TAFS on which BMSCs had been seeded for 3 days. The representative images show the live (green) and dead (red) cells. Scale bar = 200 μ m. (B) Viability analysis for the cells on TCPS, SAFS, and TAFS. (C) Comparative cell proliferation assay of BMSCs seeded on TCPS, SAFS, and TAFS. (D) In vitro evaluation of the scaffolds on osteogenesis. Representative images of ALP staining on day 7 and ARS staining on day 14 and ALP activity of BMSCs on day 7. Scale bar = 200 μ m. All values are presented as means \pm standard deviation (* P < 0.05, ** P < 0.01, *** P < 0.001, ns: P > 0.05). TCPS: tissue culture polystyrenes; SAFS: SDS-treated acellular fish scale scaffolds; TAFS: Triton X-100-treated acellular fish scale scaffolds; ALP: alkaline phosphatase staining; ARS: alizarin red staining.

(Figure 4). The elements mentioned above of NFS were homogeneously distributed on the surface. Although the decellularization process destroyed the microstructure of the surface, the distribution of elements in the scaffolds was still homogeneous.

Swelling Rate and Degradation Rate. After 48 h of water absorption and swelling, the swelling rates of each group were more than 70%. Compared with NFS, there was no significant difference in the swelling rate of each scaffold, and there was no significant difference between each scaffold (Figure 5A).

Regarding the in vitro degradation rate, the degradation rates of the scaffolds were slow in the first 4 weeks; after 4 weeks, the degradation rates accelerated significantly. At 4 weeks, the degradation rates of the scaffolds in each group

were around 8%, and at 8 weeks, the degradation rates reached around 40%. For the comparison between scaffolds, the degradation rates of SAFS and TAFS-5 were higher, of which SAFS was the highest, and the degradation rate was $49.89 \pm 6.56\%$ at 8 weeks. The degradation rates of NFS, TAFS-3, and TAFS-4 were lower, and there was no significant difference among them (Figure 5B).

Young's Modulus. We evaluated the mechanical properties of the scaffolds by measuring Young's modulus (Figure 5C). We found that Young's modulus of NFS was the highest, which was 7.80 ± 2.83 GPa. After decellularization, the Young's modulus of the scaffolds decreased to varying degrees. The Young's modulus of TAFS-3 and TAFS-4 decreased slightly to 6.26 ± 1.49 and 5.80 ± 1.17 GPa, respectively, while

that of SAFS and TAFS-5 decreased significantly to 3.63 ± 2.34 and 3.79 ± 1.28 GPa, respectively.

In Vitro Biocompatibility. After 3 days of culture, cell viability on the scaffolds was detected by Calcein-AM/PI staining. For scaffolds, most cells were stained with fluorescent green (living cells) and very few with red (dead cells; Figure 6A). Quantitative analysis showed that cell viability on the scaffolds was slightly lower than that on the TCPS, but only SAFS had a significant difference (Figure 6B). The CCK8 test showed that the cells on the scaffolds proliferated well. Compared with those of TCPS, the cell proliferation rates of scaffolds were slightly lower, but only SAFS and TAFS-3 had significant differences (Figure 6C).

In Vitro Osteogenic Differentiation. First, as a key indicator of initial osteogenic differentiation, ALP activity was assessed by ALP staining and an ALP assay kit for its expression in BMSCs on day 7. As expected, the TAFS-4 group showed the highest ALP activity (Figure 6D). Second, calcium nodule deposition, a key marker of late osteogenic differentiation, was visualized by ARS. After 14 days of culture, calcium nodules appeared in all groups, and calcium nodule deposition was the most obvious and largest in the TAFS-4 group (Figure 6D).

DISCUSSION

Currently, the treatment of bone defects remains a major challenge in the field of orthopedics. Bone tissue engineering is a bone defect repair strategy that has received increasing attention. Scaffolds, as a key to bone tissue engineering, have naturally become a research hotspot. Due to their similar composition to bone tissue, special structure, good mechanical properties, and osteogenic properties, fish scales have begun to be used in bone tissue engineering and have great potential.^{6–9} Similar to bone tissue, the fish scale-derived scaffold is composed of type I collagen and hydroxyapatite⁶ and has a highly ordered three-dimensional structure.⁷ Collagen fibers are arranged layer by layer and embedded with needle-shaped hydroxyapatite crystals, forming a unique “Bouligand” structure.⁷ These components and structures give the scaffold excellent mechanical properties, and its Young’s modulus is close to that of bone tissue.^{24,25} As the scaffold derived from biomaterials, this scaffold must undergo decellularization procedures when used in bone tissue engineering.²⁶ The decellularization process requires maximum removal of nuclei and cellular components while retaining as many natural extracellular matrix components and microstructure as possible, and the decellularization operation will inevitably affect the extracellular matrix components and native structure, so this requires striking a balance between the removal of cellular components and maintenance of the native extracellular matrix, which is one of the major challenges in tissue engineering.^{27,28} At present, there are several methods for decellularizing fish scales, some of which use highly corrosive reagents such as acetic acid²⁹ and sodium hydroxide³⁰ during the decellularization process, causing significant damage to the composition and structure of fish scales. Among them, the method using a combination of SDS and EDTA is the most widely used,^{9,10} but this method also has problems due to the ionicity and cytotoxicity of SDS.^{11–14} We optimized this method using a combined method of Triton X-100, EDTA, and nuclease, and our results verified the multiple advantages of the optimized method.

We used histological staining and DNA residence analysis to evaluate the decellularization effect at both qualitative and quantitative levels. Crapo et al.²⁸ proposed the minimum criteria that tissues should meet to be considered as successfully decellularized: (1) residual DNA content should be less than 50 ng/mg (dry weight); (2) any residual DNA fragment should be less than 200 base pairs; and (3) acellular tissue should not have visible nuclear material when stained with DAPI or H&E. Our results showed that SAFS, TAFS-4, and TAFS-5 all showed the required acellular effect, while TAFS-3 did not. Histological staining of TAFS-3 revealed nuclei and the DNA content was 50.15 ± 5.63 ng/mg. Therefore, the decellularization conditions of TAFS-3 did not meet the requirements.

Fish scales are mainly composed of hydroxyapatite and type I collagen, and their proportion is similar to that of bone tissue.⁶ These components are of great significance in the application of bone tissue engineering. Histological staining showed that the content of the extracellular matrix in fish scales decreased after decellularization. Does the optimized acellular method have an advantage in preserving the extracellular matrix? We used FTIR to quantitatively analyze the reduction of extracellular matrix components, mainly focusing on hydroxyapatite and collagen. The spectrum showed a phosphate peak ($1200\text{--}900\text{ cm}^{-1}$) and an amide I peak ($1720\text{--}1590\text{ cm}^{-1}$), representing hydroxyapatite and collagen, respectively. Similar to the reports in the literature,^{11–13} the decellularization process of SAFS not only achieved a better decellularization effect but also seriously damaged the extracellular matrix. We found that SAFS had the highest reduction ratio of hydroxyapatite and collagen contents, both exceeding 50%, while that of the optimized method was lower. The optimized method has an advantage in preserving the extracellular matrix. Studies have shown that surface topography can cause specific cell responses, such as adhesion,³¹ migration,³² proliferation, and differentiation,³³ a phenomenon known as contact guidance.³⁴ The surface of fish scales is characterized by regularly arranged ridges and grooves. This special structure may affect cell adhesion, proliferation, migration, and other important cellular behavior. Zhou et al.³⁵ prepared scaffolds derived from fish scales. After 5 days of culture, the cells on the scaffolds began to gather in the grooves. The results of DAPI fluorescence staining showed that nuclei were parallel to the grooves, indicating that the cells proliferated and migrated along the channels. It would be beneficial to preserve the surface microstructure as much as possible in the preparation of fish scale acellular scaffolds. However, SEM results showed that the surface microstructure of SAFS was seriously damaged and only TAFS-3 and TAFS-4 basically retained the surface structure. Therefore, the optimized method was better for the preservation of extracellular matrix components and the microstructure of fish scales.

Bone tissue engineering requires scaffolds to have good mechanical properties.^{2,36} Currently, various methods to improve the mechanical properties of acellular matrix scaffolds have been developed, and most of the procedures are complicated.³⁷ Fish scales themselves have excellent mechanical properties. As long as the decellularization process does not seriously damage the mechanical properties, the prepared scaffolds will have excellent mechanical properties, without complicated processing. Our results showed that the Young’s modulus of SAFS and TAFS-5 decreased obviously, while that

of TAFS-3 and TAFS-4 decreased slightly. SAFS and TAFS-5 could not well retain the extracellular matrix components and microstructure of fish scales, and accordingly, their mechanical properties would also be affected. This situation can also be found in the degradation rate because the content and structure of the extracellular matrix components were obviously destroyed, and the degradation rates of SAFS and TAFS-5 were also faster than those of other groups. Because of the ionicity and cytotoxicity of SDS, we were worried that it would have a significant impact on the cell biocompatibility. The results showed that the cell viability of each group of scaffolds was >95% and there was no statistical difference in cell proliferation among each group. However, we need to note that the cell viability and proliferation of SAFS were statistically lower than those of TCPS. We also observed that the cell proliferation of TAFS-3 was also significantly lower, which we speculated was due to the incomplete decellularization of TAFS-3 because its decellularization effect did not meet the minimum requirements. In comparison, TAFS-4 and TAFS-5 have more advantages in cell biocompatibility. The purpose of optimizing the fish scale decellularization method is to promote osteogenesis. We compared the osteogenic differentiation abilities of the scaffolds. The results showed that TAFS-4 showed the best osteogenic differentiation ability in both early and late osteogenic markers. Generally speaking, in terms of the decellularization effect, extracellular matrix composition and structure retention, mechanical properties, cell biocompatibility, and osteogenic differentiation ability, TAFS-4 was a more suitable method for decellularization of fish scales.

This study has several limitations. First, we selected only grass carp scales for our study. The scales of different fishes will be different, so our results may not be extended to other types of fish scales. Second, in this study, we only set the treatment duration of Triton X-100 as a variable to compare and optimize the fish scale decellularization scheme. More work needs to be done in the future to establish an optimal fish scale decellularization scheme. Third, for in vitro experiments, we evaluated only the effect on cell biocompatibility and osteogenic differentiation ability, and more cell studies and animal studies are needed before clinical trials. Despite these limitations, this study completed the optimization of the fish scale decellularization protocol and proposed a more suitable fish scale decellularization protocol. The acellular fish scale scaffold not only has good osteogenic induction capabilities and the advantages of easy access and low cost but also has been reported to have anti-inflammatory properties.³⁰ We will conduct further verification of the multiple characteristics of acellular fish scale scaffolds in future in vivo experiments and even clinical trials.

CONCLUSION

In summary, we combined Triton X-100, EDTA, and nuclease to optimize the current SDS-based fish scale decellularization scheme and proposed a more suitable fish scale decellularization scheme. We evaluated the decellularization effect, extracellular matrix composition and structure retention, mechanical properties, cell biocompatibility, and osteogenic differentiation ability. The decellularization process of TAFS-4 showed better results. The acellular fish scale scaffold prepared by this decellularization scheme may have great potential in bone tissue engineering.

AUTHOR INFORMATION

Corresponding Author

Fang Zhou – Department of Orthopedics, Peking University Third Hospital, 100191 Beijing, China; Engineering Research Center of Bone and Joint Precision Medicine, Peking University Third Hospital, 100191 Beijing, China; orcid.org/0000-0002-7775-069X; Email: zhouf@bjmu.edu.cn

Authors

Shilong Su – Department of Orthopedics, Peking University Third Hospital, 100191 Beijing, China; Engineering Research Center of Bone and Joint Precision Medicine, Peking University Third Hospital, 100191 Beijing, China

Ruideng Wang – Department of Orthopedics, Peking University Third Hospital, 100191 Beijing, China; Engineering Research Center of Bone and Joint Precision Medicine, Peking University Third Hospital, 100191 Beijing, China

Jinwu Bai – Department of Orthopedics, Peking University Third Hospital, 100191 Beijing, China; Engineering Research Center of Bone and Joint Precision Medicine, Peking University Third Hospital, 100191 Beijing, China

Zhengyang Chen – Department of Orthopedics, Peking University Third Hospital, 100191 Beijing, China; Engineering Research Center of Bone and Joint Precision Medicine, Peking University Third Hospital, 100191 Beijing, China

Complete contact information is available at:

<https://pubs.acs.org/10.1021/acsomega.4c05096>

Author Contributions

F. Z. and S.S. contributed to conception and experimental design. S.S., R.W., Z.C., and J.B. contributed to experimental assays and data collection. Figures were drawn by S.S. S.S. and R.W. analyzed the data and drafted the manuscript before submission. F.Z. supervised the entire process and revised the manuscript. All authors have read and approved the manuscript.

Funding

This study was supported by the National Natural Science Foundation of China (No. 81971160) and the Peking University Third Hospital Clinical Key Project Fund (No. BYSYZHKC2021106).

Notes

The authors declare no competing financial interest.

ACKNOWLEDGMENTS

The authors would like to thank Shiyanjia Lab (www.shiyanjia.com) for the AFM analysis.

REFERENCES

- (1) Guo, L.; Liang, Z.; Yang, L.; et al. The role of natural polymers in bone tissue engineering. *J. Controlled Release* **2021**, *338*, 571–582.
- (2) Koushik, T. M.; Miller, C. M.; Antunes, E. Bone Tissue Engineering Scaffolds: Function of Multi-Material Hierarchically Structured Scaffolds. *Adv. Healthc Mater.* **2023**, *12* (9), No. e2202766.
- (3) Park, J. Y.; Park, S. H.; Kim, M. G.; Park, S. H.; Yoo, T. H.; Kim, M. S. Biomimetic Scaffolds for Bone Tissue Engineering. *Adv. Exp. Med. Biol.* **2018**, *1064*, 109–121.
- (4) Amirzad, H.; Dadashpour, M.; Zarghami, N. Application of decellularized bone matrix as a bioscaffold in bone tissue engineering. *J. Biol. Eng.* **2022**, *16* (1), 1.

- (5) Cheng, C. W.; Solorio, L. D.; Alsberg, E. Decellularized tissue and cell-derived extracellular matrices as scaffolds for orthopaedic tissue engineering. *Biotechnol. Adv.* **2014**, *32* (2), 462–484.
- (6) Feng, H.; Li, X.; Deng, X.; et al. The lamellar structure and biomimetic properties of a fish scale matrix. *RSC Adv.* **2020**, *10* (2), 875–885.
- (7) Quan, H. C.; Yang, W.; Lapeyriere, M.; Schaible, E.; Ritchie, R. O.; Meyers, M. A. Structure and Mechanical Adaptability of a Modern Elasmoid Fish Scale from the Common Carp. *Matter* **2020**, *3* (3), 842–863.
- (8) Salvatore, L.; Gallo, N.; Natali, M. L.; et al. Marine collagen and its derivatives: Versatile and sustainable bio-resources for healthcare. *Mater. Sci. Eng. C Mater. Biol. Appl.* **2020**, *113*, 110963.
- (9) Wang, Y.; Kong, B.; Chen, X.; Liu, R.; Zhao, Y.; Gu, Z.; Jiang, Q. BMSC exosome-enriched acellular fish scale scaffolds promote bone regeneration. *J. Nanobiotechnol.* **2022**, *20* (1), 444.
- (10) Kara, A.; Tamburaci, S.; Tihminlioglu, F.; Havitcioglu, H. Bioactive fish scale incorporated chitosan biocomposite scaffolds for bone tissue engineering. *Int. J. Biol. Macromol.* **2019**, *130*, 266–279.
- (11) Gilpin, A.; Yang, Y. Decellularization Strategies for Regenerative Medicine: From Processing Techniques to Applications. *Biomed Res. Int.* **2017**, *2017*, 9831534.
- (12) Choi, S. H.; Chun, S. Y.; Chae, S. Y.; et al. Development of a porcine renal extracellular matrix scaffold as a platform for kidney regeneration. *J. Biomed Mater. Res. A* **2015**, *103* (4), 1391–1403.
- (13) Remaggi, G.; Barbaro, F.; Di Conza, G.; et al. Decellularization Detergents As Methodological Variables in Mass Spectrometry of Stromal Matrices. *Tissue Eng. Part C Methods* **2022**, *28* (4), 148–157.
- (14) Syed, O.; Walters, N. J.; Day, R. M.; Kim, H. W.; Knowles, J. C. Evaluation of decellularization protocols for production of tubular small intestine submucosa scaffolds for use in oesophageal tissue engineering. *Acta Biomater.* **2014**, *10* (12), 5043–5054.
- (15) Wu, W.; Zhou, Z.; Sun, G.; Liu, Y.; Zhang, A.; Chen, X. Construction and characterization of degradable fish scales for enhancing cellular adhesion and potential using as tissue engineering scaffolds. *Mater. Sci. Eng. C Mater. Biol. Appl.* **2021**, *122*, 111919.
- (16) Seddon, A. M.; Curnow, P.; Booth, P. J. Membrane proteins, lipids and detergents: not just a soap opera. *Biochim. Biophys. Acta* **2004**, *1666* (1–2), 105–117.
- (17) Liao, J.; Yang, L.; Grashow, J.; Sacks, M. S. The relation between collagen fibril kinematics and mechanical properties in the mitral valve anterior leaflet. *J. Biomech Eng.* **2007**, *129* (1), 78–87.
- (18) Chou, C. H.; Chen, Y. G.; Lin, C. C.; Lin, S. M.; Yang, K. C.; Chang, S. H. Bioabsorbable fish scale for the internal fixation of fracture: a preliminary study. *Tissue Eng. Part A* **2014**, *20* (17–18), 2493–2502.
- (19) Chen, C.; Liu, F.; Tang, Y.; et al. Book-Shaped Acellular Fibrocartilage Scaffold with Cell-loading Capability and Chondrogenic Inducibility for Tissue-Engineered Fibrocartilage and Bone-Tendon Healing. *ACS Appl. Mater. Interfaces* **2019**, *11* (3), 2891–2907.
- (20) Tang, Y.; Chen, C.; Liu, F.; et al. Structure and ingredient-based biomimetic scaffolds combining with autologous bone marrow-derived mesenchymal stem cell sheets for bone-tendon healing. *Biomaterials* **2020**, *241*, 119837.
- (21) Boskey, A.; Pleshko Camacho, N. FT-IR imaging of native and tissue-engineered bone and cartilage. *Biomaterials* **2007**, *28* (15), 2465–2478.
- (22) Khanarian, N. T.; Boushell, M. K.; Spalazzi, J. P.; Pleshko, N.; Boskey, A. L.; Lu, H. H. FTIR-I compositional mapping of the cartilage-to-bone interface as a function of tissue region and age. *J. Bone Miner. Res.* **2014**, *29* (12), 2643–2652.
- (23) Zhou, Y.; Chen, C.; Guo, Z.; Xie, S.; Hu, J.; Lu, H. SR-FTIR as a tool for quantitative mapping of the content and distribution of extracellular matrix in decellularized book-shape bioscaffolds. *BMC Musculoskelet Disord* **2018**, *19* (1), 220.
- (24) Yang, W.; Quan, H. C.; Meyers, M. A.; Ritchie, R. O. Arapaima Fish Scale: One of the Toughest Flexible Biological Materials. *Matter* **2019**, *1* (6), 1557–1566.
- (25) Bruet, B. J. F.; Song, J. H.; Boyce, M. C.; Ortiz, C. Materials design principles of ancient fish armour. *Nat. Mater.* **2008**, *7* (9), 748–756.
- (26) Kim, Y. S.; Majid, M.; Melchiorri, A. J.; Mikos, A. G. Applications of decellularized extracellular matrix in bone and cartilage tissue engineering. *Bioeng. Transl. Med.* **2019**, *4* (1), 83–95.
- (27) Aamodt, J. M.; Grainger, D. W. Extracellular matrix-based biomaterial scaffolds and the host response. *Biomaterials* **2016**, *86*, 68–82.
- (28) Crapo, P. M.; Gilbert, T. W.; Badylak, S. F. An overview of tissue and whole organ decellularization processes. *Biomaterials* **2011**, *32* (12), 3233–3243.
- (29) Chen, L.; Cheng, G.; Meng, S.; Ding, Y. Collagen Membrane Derived from Fish Scales for Application in Bone Tissue Engineering. *Polymers* **2022**, *14* (13), 2532.
- (30) Lin, X.; Kong, B.; Zhu, Y.; Zhao, Y. Bioactive Fish Scale Scaffolds with MSCs-Loading for Skin Flap Regeneration. *Adv. Sci.* **2022**, *9* (21), No. e2201226.
- (31) Khang, D.; Lu, J.; Yao, C.; Haberstroh, K. M.; Webster, T. J. The role of nanometer and sub-micron surface features on vascular and bone cell adhesion on titanium. *Biomaterials* **2008**, *29* (8), 970–983.
- (32) Jeon, H.; Koo, S.; Reese, W. M.; Loskill, P.; Grigoropoulos, C. P.; Healy, K. E. Directing cell migration and organization via nanocrater-patterned cell-repellent interfaces. *Nat. Mater.* **2015**, *14* (9), 918–923.
- (33) Gittens, R. A.; McLachlan, T.; Olivares-Navarrete, R.; et al. The effects of combined micron-/submicron-scale surface roughness and nanoscale features on cell proliferation and differentiation. *Biomaterials* **2011**, *32* (13), 3395–3403.
- (34) Zhu, M.; Ye, H.; Fang, J.; et al. Engineering High-Resolution Micropatterns Directly onto Titanium with Optimized Contact Guidance to Promote Osteogenic Differentiation and Bone Regeneration. *ACS Appl. Mater. Interfaces* **2019**, *11* (47), 43888–43901.
- (35) Fang, Z.; Wang, Y.; Feng, Q.; Kienzle, A.; Muller, W. E. Hierarchical structure and cytocompatibility of fish scales from *Carassius auratus*. *Mater. Sci. Eng. C Mater. Biol. Appl.* **2014**, *43*, 145–152.
- (36) Peng, Z.; Zhao, T.; Zhou, Y.; Li, S.; Li, J.; Leblanc, R. M. Bone Tissue Engineering via Carbon-Based Nanomaterials. *Adv. Health Mater.* **2020**, *9* (5), No. e1901495.
- (37) Jiang, S.; Wang, M.; He, J. A review of biomimetic scaffolds for bone regeneration: Toward a cell-free strategy. *Bioeng. Transl. Med.* **2021**, *6* (2), No. e10206.